PROCEEDINGS, Twenty-Third Workshop **on Geothermal Reservoir Engineerine**
Stanford University, Stanford, California, January 26–28, 1998
SGP-TR-158

ANALYSIS OF PRODUCTION/INJECTION DATA FROM SLIM HOLES AND LARGE-DIAMETER WELLS AT THE KIRISHIMA GEOTHERMAL FIELD. JAPAN

Sabodh. K. Garg
Maxwell Technologies
San Diego, California

Jim Combs
Geo Hills Associates
Los Altos Hills, California

Makio Kodama and Kazunori Gokou
Nittetsu Kagoshima Geothermal Co., Ltd
Tokyo, Japan

ABSTRACT

A majority of Kirishima boreholes produced from liquid feedzones. Production and injection data from boreholes with liquid feedzones imply that (1) productivity and injectivity indices are more or less equal and (2) discharge rate of large-diameter wells may be predicted based on test data from slim holes. These conclusions are in agreement with those derived from analyses of similar data from Oguni, Takigami, Sumikawa and Steamboat Hills Geothermal Fields. Analysis of injection and production data from boreholes with two-phase feedzones from Oguni, Sumikawa and Kirishima Geothermal Fields indicates that the two-phase productivity index is about an order of magnitude smaller than the injectivity index. A wellbore simulator was used to examine the effect of borehole diameter on the discharge capacity of geothermal boreholes with two-phase feedzones.

INTRODUCTION

The U.S. Department of Energy (DOE) through Sandia National Laboratories (Sandia) initiated a research effort to demonstrate that slim holes can be used (1) to provide reliable geothermal reservoir parameter estimates comparable to those obtained from large-diameter wells, and (2) to predict the discharge behavior of large-diameter wells (Combs and Dunn, 1992). As part of the DOE/Sandia slim hole research program, production and injection data from slim holes and large-diameter wells at four geothermal fields (Oguni, Japan; Sumikawa, Japan; Takigami, Japan; and Steamboat Hills, U.S.A.) have been analyzed by Garg and Combs (1997) in order to establish relationships (1) between injectivity and productivity indices, (2) between productivity/injectivity index and borehole diameter, and (3) between discharge capacity of slim holes and large-diameter wells. Based on the examination of these data, the productivity and injectivity indices for boreholes with liquid feedzones are more or less equal. Except for Oguni boreholes, the productivity and injectivity indices display no correlation with borehole diameter. Thus, the productivity index (or, more importantly, the injectivity index in the absence of discharge data) from a slim hole with a liquid feed can be used to provide a first estimate of the probable discharge capacity of a large-diameter geothermal production well. The large-diameter wells at the Oguni, Sumikawa and Steamboat Hills Geothermal Fields have a more or less uniform inside diameter; and the discharge capacity of these wells (with liquid feedzones) can be predicted using Pritchett's (1993) "scaled maximum discharge rate" in conjunction with discharge data from slim holes. Because of the non-uniform internal diameter for large-diameter Takigami wells, a numerical simulator was used to model the available discharge data from Takigami boreholes. The results of numerical modeling indicate that the flow rate of large-diameter Takigami production wells with liquid feedzones can also be predicted using discharge and injection data from slim holes (Garg and Combs, 1997).

Currently available data and analyses are insufficient to predict the discharge characteristics of large-diameter wells with two-phase feeds based on slim hole data. Because of relative permeability effects in two-phase flow, the productivity index (with ***in situ*** boiling) is likely to be much smaller than the injectivity index. Additional studies are required to understand relationships (1) between injectivity index and two-phase productivity index, (2) between borehole diameter and two-phase productivity index, and (3) between well completion (*i.e.*, diameter) and the discharge capacity of boreholes with two-phase feedzones.

In the present paper, the analysis of data from slim holes and large diameter wells at the Kirishima Geothermal Field, Southern Kyushu, Japan, is presented. Since 1972, Nittetsu Mining Company (NMC), Nippon Steel Corporation (NSC), Nittetsu Kagoshima Geothermal Company (NKGC) and the Japanese government through the New Energy and Industrial Technology Development Organization (NEDO) and the Geological Survey of Japan (GSJ) have carried out an extensive exploration and reservoir assessment program in the area. From detailed analysis of geological information, geophysical logging and well tests, NKGC confirmed

that the Kirishima reservoir of the Ginyu/Ogiri fault zone is sufficient for supplying a geothermal power plant of 30 MW capacity (Kodama and Gokou, 1995). On March 1, 1996, the Ogiri Geothermal Power Plant (30 MW), owned and operated by Kyushu Electric Power Co., Ltd., was inaugurated and began commercial production.

A brief overview of the Kirishima Geothermal Field is presented in the next section. The feedzone pressures (and temperatures) for individual boreholes imply the existence of two separate "reservoirs" based on the fact that the feedzone pressures for most of the Ginyu and Shiramizugoe boreholes lie along two separate trendlines. Estimates of injectivity and productivity indices are presented next. Relationships between the productivity and injectivity indices of slim holes and of large-diameter wells with liquid feedzones and two-phase feedzones are also explored. Characteristic discharge data and variation of maximum discharge rate with borehole diameter are discussed. Mathematical modeling of fluid flow in boreholes with two-phase feedzones from the Oguni, Sumikawa, and Kirishima Geothermal Fields is also presented. Finally, the conclusions and recommendations for geothermal reservoir evaluation using discharge and injection data from slim holes are outlined.

KIRISHIMA GEOTHERMAL FIELD

The Kirishima Geothermal Area is located in the Kagoshima Prefecture of southern Kyushu, Japan, in the Kagoshima graben (a volcano-tectonic depression) which trends from NNE to SSW. Kagoshima graben contains several active volcanoes, fumaroles, numerous hot springs, and hydrothermal alteration halos. Geothermal exploration of the Kirishima area was commenced in 1972 by NMC with conducting of surficial geological surveys, electrical soundings, heat measurement surveys and 30m-deep heat flow holes. Based on the results of these exploratory surveys, NMC and **NSC** drilled twenty-three (23) exploratory boreholes, of which eight (8) were slim holes and the other fifteen (15) large-diameter wells (see Figure 1 for borehole locations). During the time period from 1975 to 1985, NEDO drilled an additional fifteen (15) exploratory slim holes in and around the immediate vicinity of the Kirishima Geothermal Field. After 1985, the geothermal exploration has been focused on the Ginyu fault area which occupies a northern section of the Kirishima area, covering about 1 km by 2 km in areal extent. NKGC drilled sixteen (16) large-diameter production and injection wells in the Ginyu area during 1990 and 1991.

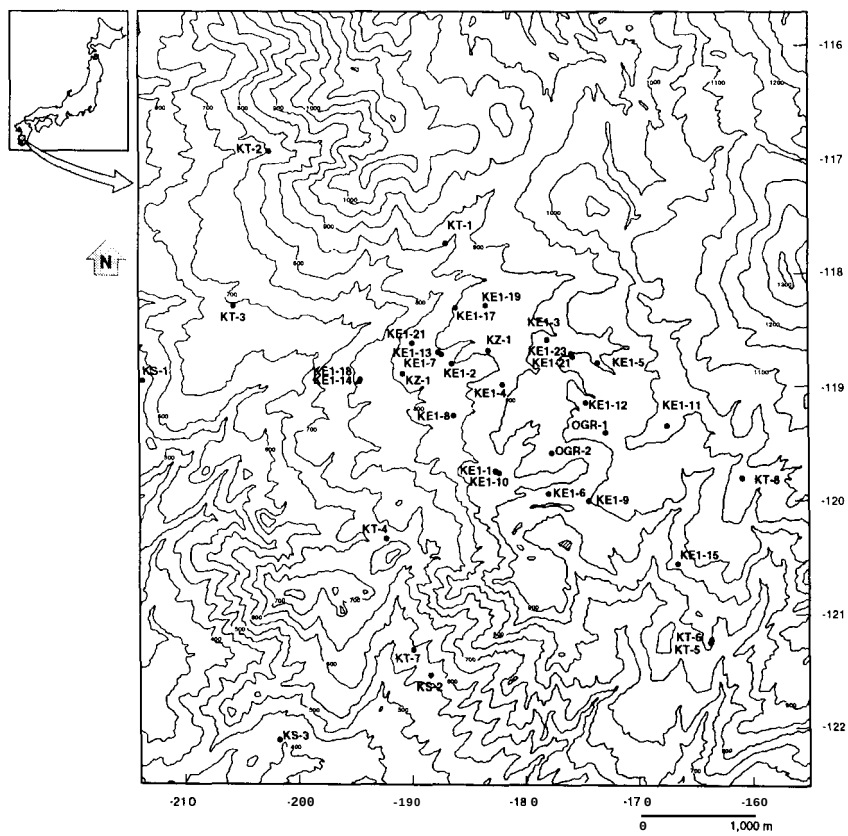

Figure 1. **A** topographic map of the Kirishima borefield. The location of the Ginyu fault zone is roughly coincident with a line passing through KE1-7 and KE1-17. The inset map of Japan shows the location of the Kirishima Geothermal Field.

Of the fifty-four (54) boreholes, including redrills, the total depths range from about 500 to 2000 meters. The deepest borehole in the Kirishima field (slim hole KE1-4) was drilled to a total depth of about 2000 meters. The production wells in the Ginyu fault zone, supplying the Ogiri Geothermal Power Plant, have a base temperature of about 230°C and the feedzones are situated between about 1100 and 1350 meters true vertical depth. The reservoir fluid in the Kirishima Geothermal Field is single-phase liquid at feedzone depth for most of the boreholes; thus, discharge from both the slim holes and large-diameter wells does not lead to *in situ* boiling. However, two-phase conditions seem to exist at shallow depths in the Ginyu fault zone and the discharge from two slim holes and one large-diameter well is accompanied by *in situ* boiling. Outside the Ginyu fault zone, the formation permeability is low, and well discharge often leads to *in situ* boiling.

NKGC has used numerous cores, as well as drilling and geophysical logs to delineate the geological sequence. In order of increasing depth (see Figure 2), these formations in the Kirishima area are the following (Gokou, *et al*., 1988; Saga and Nobumoto, 1988):

Older Kirishima Volcanic Rocks: Late Pleistocene to Recent (0.13 - 0.60 Ma), consist of *Old Shiratori Luva* (andesitic lava flows and pyroclastics), and *Takahara Conglomerate* (pyroclastics and minor lake deposits).

Kakkuto Andesites: Pleistocene (0.23 - 1.21 Ma), consist of three separate lavas, *i.e.*, *Kurino Lava*, *Sagari Lava,* and *Makizono Lava.*

Ebino Formation/Iino Lava: Early Pleistocene (1.37 Ma), fractured and permeable units.

Kirishima Welded Tuff Early Pleistocene (1.50 - 2.3 Ma), pyroclastics and welded tuffs.

Shimanto Supergroup: Tertiary (>25.0 Ma), basement in the Kirishima area, highly decomposed, mainly consisting of sandstones and shales.

Most of the feedzones for the Kirishima boreholes tend to align along the faults and are located in the Makizono lavas, Ebino formation and Iino lavas. The most important faults (Gokou, *etal.*, 1988) in the Kirishima Geothermal Area (see Figure *2)* are the Ginyu fault (ENE-WSW strike, dipping to NW) and the Shiramizugoe fault (ENE-WSW strike, dipping to SE). Many boreholes were drilled along these faults in an attempt to find high-temperature, permeable horizons (Kodama and Nakajima, 1988).

The stable shutin feedzone pressures for the Kirishima boreholes are presented in Figure 3. The feedzone pressures for most of the Ginyu/Ogiri and Shiramizugoe boreholes lie along two trendlines. The vertical pressure gradient for the Ginyu/Ogiri area is 7.792 kPa/m and corresponds to a hydrostatic gradient at 253°C. Since the reservoir temperatures in the area are only

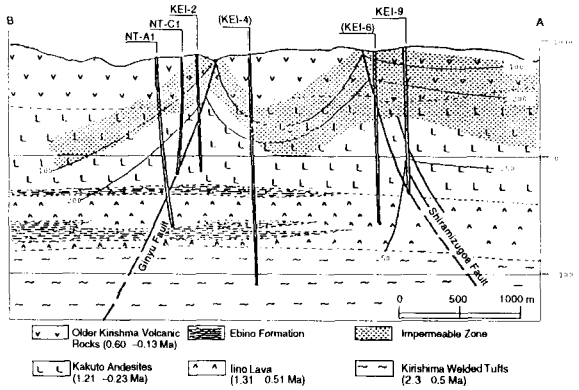

Figure 2. A generalized northwest-southeast geologic cross-section through the Kirishima geothermal field. Temperature contours (50°C interval) are also shown.

about 230°C, it is likely that the Ginyu fault zone is a downflow zone of the Kirishima Geothermal Field. The reservoir pressure in the Shiramizugoe area is about 15 bars higher than that in the Ginyu/Ogiri area, indicating that these reservoirs are separated by an impermeable barrier. For the Shiramizugoe fault zone, the vertical pressure gradient is 8.298 kPa/m and corresponds to a hydrostatic gradient at about 215°C. Since the reservoir temperatures in the Shiramizugoe area are considerably higher than 215°C, it is reasonable to conclude that fluid upwelling is taking place in the Shiramizugoe area.

The temperature distribution along a northwest-southeast plane in the Kirishima Geothermal Area on a geological cross-section is shown in Figure 2. Temperatures in the Ginyu fault zone large-diameter production wells (NT-A1 and NT-C1) are about 230°C. The temperature increases toward the southeast near the Shiramizugoe fault zone, with the maximum temperature (–250°C) in the area occurring near the Kirishima exploratory large-diameter well KE1-9. The highest temperature (~298°C) at Kirishima was recorded in slim hole N56-KT-8 (see Figure 1) located to the east of the Shiramizugoe fault zone.

The reservoir fluid in the Kirishima Geothermal Field is single-phase liquid at feedzone depth for most of the boreholes; however, two-phase conditions appear to exist at shallow depths throughout the area. The permeability in the Ginyu fault zone is sufficiently high to preclude *in situ* boiling during discharge. Outside the Ginyu fault zone (and possibly parts of the Shiramizugoe fault zone), the formation permeability is low, and borehole discharge often leads to *in situ* boiling.

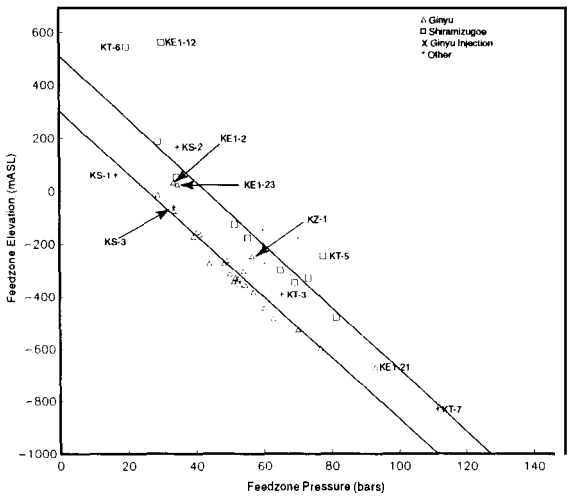

Figure 3. Feedzone pressure versus feedzone elevations for Kirishima boreholes. The straight lines are trend lines (drawn by eye) for Ginyu/Ogiri and Shiramizugoe boreholes.

Based on the examination of fluids obtained from six (6) boreholes , the Kirishima reservoir fluid composition is of the near-neutral pH Na-K-Cl-SO4 type (Shimizu, ***et*** *al.*, 1988; Kodama and Nakajima, 1988). The Ginyu boreholes have an average chloride concentration of ~ 650 mg/l, while the Shiramizugoe borehole has a chloride concentration of 1075 mg/l. The value of pH for most of the boreholes in the Kirishima Geothermal Area range from 5.46-7.57; however, a few of the boreholes in the Shiramizugoe area discharge acidic fluids and have pH values of 2.4 to 2.9. The gas content of fluids discharged from Kirishima boreholes is less than 0.6 mmol/mol. Carbon dioxide constitutes the bulk of the non-condensable gases in the reservoir fluid.

As discussed earlier, most of the feedzones for the Kirishima boreholes tend to align along the faults and are located in the Makizono lavas, Ebino formation and Iino lavas. Like most volcanic geothermal areas, permeability in the Kirishima Geothermal Field is due primarily to the pervasive network of fractures. Most of the boreholes have no feedzones in the upper and middle Makizono lavas which have undergone extensive hydrothermal alteration; and therefore, this relatively impermeable region of the Makizono lavas acts as a caprock for the Ginyu/Ogiri reservoir. Based on pressure transient testing, the transmissivity (*i*.e., permeability-thickness product) for the Ginyu/Ogiri reservoir is estimated to be 40 darcy-meters (Kitamura, *et al.*, 1998). The discharge and injection testing data indicate that the transmissivity in the Shiramizugoe reservoir is less than for the Ginyu/Ogiri reservoir.

INJECTION AND DISCHARGE TESTS

Injection tests have been performed on eighteen (18) slim holes and eleven (11) large-diameter wells at Kirishima. Injection tests are usually carried out either prior to or soon after the drilling and completion of a borehole. **A** typical injection test at Kirishima consists of injecting cold water into a borehole at a fixed rate and simultaneously monitoring pressure downhole. In most cases, injection was performed using two or more different rates. During the injection tests, the downhole pressure tool (Kuster gauges), in several cases, was placed substantially above the feedzone depth. Because of wellbore cooling due to the injection of cold fluid, the measured change in pressure at the gauge depth will underestimate the change in pressure at the feedzone depth. The discrepancy in rates of pressure change at the gauge and feedzone depths will decline with continued injection. After the injection of a few wellbore volumes, the temperature in the depth interval between the gauge and feedzone depths should approach a stable value; hence, the rates of pressure change at the two depths will be similar. The injectivity index **(11)** is defined as follows:

$$II = \frac{M}{P_{flowing} - P_{static}} \qquad (4.1)$$

where M is the injection rate (single rate test), $P_{flowing}$ is the flowing pressure (at gauge depth) during cold water injection, and P_{static} is the shut-in pressure at the gauge depth. For multi-rate injection tests, Equation (4.1) can be rewritten as follows:

$$II = \frac{\Delta M}{\Delta P} \qquad (4.2)$$

where $\Delta M/\Delta P$ is the slope of the straight-line fit to the multi-step injection rate versus injection pressure (at gauge depth) data. The injectivity data are summarized in Table 1.

Ten (10) slim holes and sixteen (16) large-diameter wells have been discharged at one time or another. At Kirishima, the permeable intervals are associated with Ginyu and Shiramizugoe fault zones; elsewhere, the permeability is generally poor. Most of the Ginyu/Ogiri boreholes, drilled into the Ginyu fault zone, produce from liquid feedzones. Discharge from boreholes located outside the fault zones is in most cases accompanied by ***in situ*** boiling. With the exception of two (2) slim holes (54E-OGR-1 and N55-KT-5) and one (1) large-diameter well (KE1-19), downhole pressure surveys were run during the discharge tests of various Kirishima boreholes. For about half the boreholes, multi-rate discharge tests were performed, and pressures were recorded downhole with capillary tube type

gauges. These pressure data can be used to determine the productivity index as follows:

$$PI = \frac{\Delta M}{\Delta P} \qquad (4.3)$$

where $\Delta M/\Delta P$ is the slope of the straight-line fit to the multi-step discharge rate versus flowing pressure (at gauge depth) data.

Downhole pressure gradient surveys were run in approximately half of the boreholes during discharge tests. The pressure gradient data can be used to calculate the flowing feedzone pressure (P_{fp}) and the productivity index. PI.

$$PI = \frac{M}{P_{ns} - P_{fp}}. \qquad (4.4)$$

Table 1. Injectivity Indices for Kirishima Boreholes.

Borehole Name	Open Hole Diameter (mm)	Feedzone Depth (mTVD)	Test Date(s)	Pressure Gauge Depth (mTVD)	Injectivity Index (kg/s-bar)	Remarks
50-KS-1	81	460	05-07-76 05-07-76	431.8 431.8	0.47 0.41	
50-KS-3	79	465	01-26-76	297.2	0.69	
54E-OGR-1	101	1145	09-19-80	645.0	0.11	
54E-OGR-2	101	745	06-03-80	360.0	0.46	
N55-KT-1	100	1210	10-07-81	1300.0	0.34	
N55-KT-2	101	915	09-07-81	600.0	0.24	
N55-KT-3	101	1085	07-07-81	632.0	0.04	
N55-KT-4	98	1160	09-07-81	900.0	0.83	
N55-KT-5	101	1100	06-07-81	1076.0	0.78	
N56-KT-7	99	1425	06-07-82	1350.0	0.69	
N56-KT-8	100	1380	05-07-78	1500.0	1.11	
N59-KZ-1	76	1120	07-18-85	1120.0	0.05	
N60-KZ-2	101	1410	03-22-86	1400.0	0.07	
KE1-1	78	830	08-29-80 08-30-80	700.0? 790.0	0.22 0.11	Before 73 mm liner. After 73 mm liner.
KE1-3	79	1170	06-16-81	800.0	0.72	
KE1-4	98	1400	08-03-83 08-04-83	1350.0 1760.0	2.43 3.63	
KE1-5	102	1260	04-02-83	1250.0	1.64	
KE1-6	98	1235	04-05-83	1400.0	1.15	
KE1-7 (NT-C1)	216	920	02-04-83	850.0	8.81	
KE1-12	216	410	01-23-84	300.0	2.13	
KE1-14 (NT-D1)	270	550	06-21-84	700.0	4.93	Inj. water temp 89°C.
KE1-18 (NT-D2)	216	860	11-21-85 02-07-86	715.3 678.1	3.94 1.33	Inj. water temp 86°C.
NT-D3	216	910	10-19-90	916.8	1.24	
NT-D4	216	940	? ? ?	356.0 943.5 943.5	2.04 4.37 5.49	Inj. water temp. 85°C. Inj. water temp. 85°C.
NT-D5	216	1035	06-13-91	467.7	1.80	
NT-E1	216	930	? ?	400.0 850.7	3.47 5.62	Inj. water temp. 85°C.
NT-E2	216	1045	05-29-91	1039.8	1.26	Inj. water temp. 85°C.
NT-E3	216	960	07-17-91	951.2	1.00	Inj. water temp. 85°C.
NT-E4	216	870	07-24-91	450.0	1.49	

Here P_{ns} is the stable feedzone pressure. Boreholes completed in the Ginyu fault zone have large productivity indices, and production from these boreholes is accompanied by little or no pressure drop. Because of the inherent limitations of Kuster tools (resolution, accuracy, calibration) employed at Kirishima, the use of pressure gradient surveys to compute productivity indices for high-permeability Ginyu/Ogiri boreholes is problematical. The productivity indices for the Kirishima boreholes are summarized in Table 2.

Table 2. Productivity Indices for Kirishima Boreholes.

Borehole Name	Open Hole Diameter (mm)	Gauge Depth (mTVD)	Test Date(s)	Discharge Rate (kg/s)	Static Pressure (bar)	Flowing Pressure (bar)	Productivity Index (kg/s-bar)
N56-KT-8	100	1380.0	02-24-83 – 02-26-83	5.64 – 8.31	–	64.85 – 64.17	3.94
N60-KZ-2	101	1340.0	06-01-86	1.5	69.5	28.5	0.04
KE1-1	78	830.0	12-18-80	1.25	34.4	7.2	0.05*
KE1-2	75	810.0	08-10-81	1.78	33.6	14.1	0.09*
KE1-3	79	1170.0	09-01-81 – 09-03-81	4.22 – 5.83	49.3	32.7 – ---	0.36
KE1-4	98	1500.0?	02-05-84	9.72	79.02	76.67	4.14
KE1-5	102	1260.0	06-18-83 06-19-83	7.06 77.5	54.1	41.6 39.9	0.55
KE1-6	98	1235.0	07-09-83	2.73 2.75	73.2	21.4 16.5	0.05* 0.05*
KE1-7 (NT-C1)	216	920.0	06-02-83	21.51	33.8	28.9	4.39
KE1-9	216	1230.0	06-30-84	17.2	65.0	33.2	0.54*
KE1-11	216	1130.0	05-31-84	18.3	51.5	52.6	Large
KE1-17 (NT-A1)	216	1130.0	04-04-86	25.8	48.5	48.35	170.00
KE1-19S	159	1260.0	09-01-86 09-16-86	23.9 14.5	–	57.88 58.00	78.00
KE1-21	216	1635.0	02-22-86 02-27-86	3.75 3.39	93.0	15.2 10.9	0.05* 0.04*
KE1-22 (NT-C2)	216	1000.0	02-11-86 02-25-86	25.0 48.0	39.4	40.4 40.5	Large
KE1-23	216	940.0	08-05-86	11.4	34.8	9.3	0.45*
NT-A2	216	1313.9	11-02-90 – 11-25-90	16.4 – 62.8	–	62.69 – 62.50	300.00
NT-A3	216	1187.1	01-11-91 – 02-11-91	11.1 – 58.5	–	52.06 – 51.94	400.00
NT-A4	216	1337.6	05-30-91 – 06-08-91	20.0 – 46.0	–	65.64 – 65.45	190.00
NT-B1	216	1196.6	11-14-90 – 12-15-90	23.8 – 63.3	–	54.65 – 54.58	550.00
NT-B2	216	1113.5	02-20-91 – 03-01-91	16.0 – 64.8	–	47.65 – 47.41	200.00
NT-B3	216	1194.8	04-19-91 – 04-26-91	11.4 – 47.2	–	5451 – 51.90	14.30
NT-B4	216	1155.7	07-06-91 – 07-14-91	14.9 – 43.7	–	50.48 – 50.15	150.00

*Two-phase flow.

Discharge capacity of a geothermal borehole is principally determined by pressure losses associated with flow (1) in the reservoir rocks, and (2) in the welibore. Ignoring pressure transient effects, the flow resistance (or pressure losses) of the reservoir rock can be characterized by the productivity index. Prediction of the mass output of a large-diameter well based on discharge data from a slim hole requires, among other things, a relationship between productivity index and borehole diameter.

Because of the increased importance of frictional and heat losses in small-diameter boreholes, it is often difficult to discharge slim holes. There is, however, no problem with performing injection tests and determining injectivity index on slim holes. If a relationship can be established between injectivity and productivity indices, then it should be possible to use injection tests on slim holes to predict the probable discharge characteristics of large-diameter wells.

Based on theoretical considerations, Pritchett (1993) and Hadgu, et *al.* (1994) have suggested that the productivity (or injectivity) index should exhibit only a weak dependence on borehole diameter. Unfortunately, the Kirishima data are not well-suited for ascertaining the effect of borehole diameter on the injectivity/productivity index. Most of the slim holes – drilled early on during the exploration phase – are located in the less permeable parts of the reservoir. A large fraction of the large-diameter production/injection wells were drilled to intersect the extremely permeable Ginyu fault zone; large-diameter wells have very large (> 50 kg/s-bar) productivity indices. Only one Ginyu/Ogiri production well (KE1-7/NT-C1) has a productivity index less than 10 kg/s-bar.

In contrast with the Ginyu/Ogiri production wells, the large-diameter injection wells (KE1-14, KE1-18, NT-D3, NT-D4, NT-D5, NT-E1 ,NT-E2, NE-3, NT-E4) have modest (1 kg/s-bar to 5 kg/s-bar) injectivity indices. Slim holes N56-KT-8, KE1-4, KE1-5, and KE1-6, have injectivity indices greater than 1 kg/s-bar. Disregarding the slim holes drilled by the Japanese government agencies, it can be argued that the injectivity indices for Kirishima boreholes (Table1) do not display a systematic correlation with borehole diameter. The latter result is in agreement with the results for Takigami and Sumikawa boreholes, but is at variance with the injectivity/productivity indices for Oguni boreholes (Garg and Combs, 1997). Both the productivity and injectivity indices for Oguni boreholes display a strong dependence on borehole diameter. Garg, *et al.* (1995) ascribed the apparent variation of productivity/injectivity indices with borehole diameter to differences in drilling techniques (*i.e.*, core drilling versus rotary drilling). The injectivity and productivity index data for Takigami, Sumikawa, and Kirishima boreholes, however, indicate that core drilling (with complete circulation loss) did not result in any impairment of borehole injectivity/productivity. Thus, it is unlikely that enhanced formation plugging in boreholes drilled with coring rigs is a pervasive phenomenon.

Injection tests for three boreholes (KE1-18, NT-D4, and NT-El) were performed with both cold water (~0°C) and hot water (~85°C). Although the viscosity of water at 85°C is significantly less than that at 0°C, the injectivity indices display no significant correlation with the temperature of the injected water. This result is consistent with the observation that the injectivity and productivity indices for boreholes with liquid feedzones are more or less equal (Garg and Combs, 1997). Apparently, the resistance of the reservoir rocks to fluid flow is determined by the in situ fluid temperature.

Both productivity and injectivity indices are available for seven (7) slim holes and one (1) large-diameter well at Kirishima. Five (5) slim holes (KT-8, KZ-2, KE1-3, KE1-4,KE1-5) and the single large-diameter well ((KE1-7) discharge from liquid feedzones. Discharge from two (2) Kirishima slim holes (KE1-I, KE1-6) is accompanied by in situ boiling. Injectivity and productivity indices for Kirishima, Oguni, Sumikawa, and Takigami boreholes with liquid feedzones are displayed in Figure 4. Like the Oguni, Sumikawa, and Takigami geothermal boreholes with liquid feedzones, the productivity and injectivity indices for Kirishima boreholes are equal to first order. Based upon the rather large volume of data displayed in Figure 4, it is reasonable to conclude that, in the absence of discharge testing, the injectivity index may be used to compute the flow resistance of naturally fractured geothermal formations to liquid production.

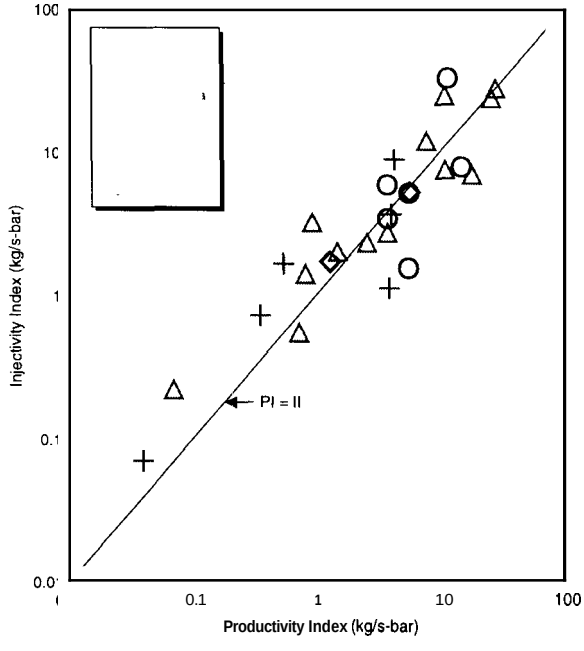

Figure 4. Injectivity index (11) versus productivity index (PI) for Kirishima, Oguni, Sumikawa, and Takigami boreholes with liquid feedzones.

It is apparent from Table 3 that the productivity index for a borehole with *in* situ boiling is much smaller than the injectivity index. Because of relative permeability effects, the flow resistance of reservoir rocks is much greater for two-phase flow than single-phase liquid transport. The injectivity and productivity (with two-phase flow) index data for Oguni, Sumikawa, and Kirishima boreholes are exhibited in Figure *5.* The data in Figure 5 suggest that the productivity index for two-phase transport is approximately one-tenth of the corresponding injectivity index. Because of the sparseness of the data set the latter conclusion must be regarded

as tentative. Additional studies are required to draw firm conclusions regarding the relationship between injectivity index and two-phase productivity index. Data from high-temperature geothermal fields spanning a wide range of transmissivities are needed for these studies.

Table 3. Productivity/Injectivity Indices for Oguni, Sumikawa, and Kirishima Boreholes With Two-Phase Feedzones.

Geothermal Field	Borehole	Final Diameter (mm)	Productivity Index (PI) (kg/s-bar)	Injectivity Index (II) (kg/s-bar)	II/PI
Oguni	GH-15	216	0.25	1.75	7.0
Sumikawa	S-2(i)	101	0.03	0.76	25.0
Sumikawa	S-4	159	0.94	1.4	1.5
Sumikawa	SA-1	216	0.16	1.5	9.0
Sumikawa	SA-4	216	0.11	0.94	9.0
Kirishima	KE1-1	78	0.05	0.16	3.0
Kirishima	KE1-6	98	0.05	1.15	23.0

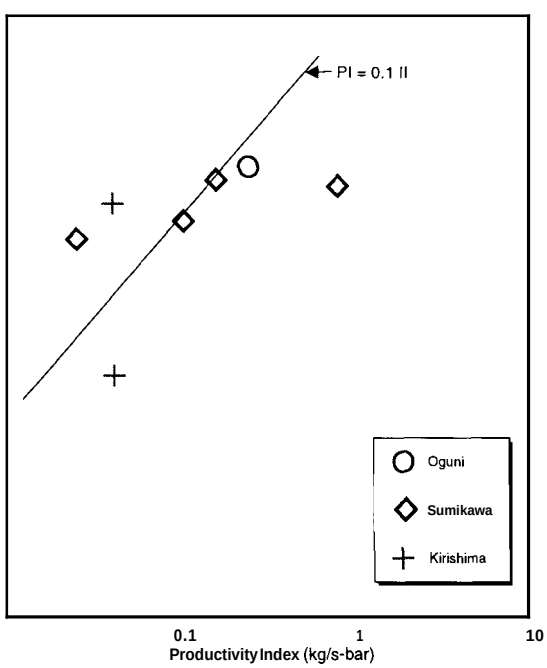

Figure 5. Injectivity index (11) versus productivity index (PI) for Kirishima, Oguni and Sumikawa boreholes with two-phase feedzones.

DISCHARGE CAPACITY AND BOREHOLE DIAMETER

A total of ten (10) slim holes have been discharged at Kirishima. The discharge data are required to determine the characteristics output curves (i.e., mass and enthalpy versus wellhead pressure). Downhole pressure/temperature surveys and wellhead enthalpy measurements indicate that discharge from five slim holes (54E-OGR-1, N55-KT-5, KEI-1, KEI-2 and KE1-6) and four large-diameter wells (KE1-9, KE1-19, KE1-21 and KE1-23) is accompanied by *in situ* boiling; the remaining boreholes at Kirishima produce from liquid feedzones. Slim holes 54E-OGR-1, N60-KZ-2, KEl-1 and KE1-2 were discharged for only brief periods; thus, these boreholes did not attain a stable discharge rate during the test period. Consequently, these slim holes are not considered in the following discussion.

The fluid carrying capacity of geothermal boreholes of varying sizes has been investigated by Pritchett (1993) and Hadgu, et al. (1994). Pritchett (1993) carried out numerical simulations assuming that (1) boreholes are of uniform size, (2) pressure losses in the formation are negligible, and (3) boreholes produce from a liquid feedzone. According to Pritchett (1993), the maximum discharge rate of a borehole, M_{max}, increases at a rate somewhat greater than the square of borehole diameter, i.e.,

$$M_{max} = M_0 (d/d_0)^{2+n}, \; n > 0$$

$$= M^* (d/d_0)^n$$

where M_{max} (M_0) denotes the discharge rate of a borehole with internal diameter $d(d_0)$. The area-scaled discharge rate M^* is defined as follows:

$$M^* = M_0 (d/d_0)^2.$$

The value of n may reasonably be expected to vary with feedzone conditions (depth, pressure, temperature, gas content) and well completion (slotted liner, or unlined, uniform or non-uniform internal diameter). For the conditions assumed by Pritchett (feedzone depth = 1500 m, pressure = 80 bars, single phase liquid at 250°C, and uniform internal diameter), n is approximately equal to 0.56.

Garg and Combs (1997) have examined production data from slim holes and large-diameter wells in four geothermal fields (Oguni, Japan; Sumikawa, Japan; Steamboat Hills, **U.S.A.;**Takigami, Japan) to determine the effect of borehole diameter on the discharge rate. Most of the Oguni, Sumikawa and Steamboat Hills boreholes have a more or less uniform internal diameter, and thus, satisfy one of the key assumptions (*i.e.*, uniform wellbore diameter) invoked by Pritchett. For boreholes with liquid feedzones in the Oguni, Sumikawa and Steamboat Hills geothermal fields, the "scaled maximum discharge rate" provides a reasonable estimate of the maximum discharge rate of large-diameter geothermal wells based on discharge data from slim holes. The large-diameter production wells at Takigami have non-uniform internal diameter; and therefore, Pritchett's scaling rule does not apply to Takigami boreholes. Garg and Combs (1997) used a wellbore simulator to explore the relationship between the discharge capacity of slim holes and large-diameter Takigami wells. Based on these

numerical calculations, they concluded that the discharge characteristics of large-diameter wells may be predicted using discharge data for slim holes with liquid feedzones.

With the single exception of slim hole KE1-3, all of the Kirishima boreholes with liquid feedzones have a more or less uniform internal diameter. The "area-scaled" and "scaled maximum (n = 0.56)" discharge rates for the Kirishima slim holes (liquid feedzones) are compared with measured discharge rates for large-diameter wells at Kirishima in Table 4. For the sake of clarity, the Ginyu and Shiramizugoe area boreholes are listed separately. Slim hole N60-KZ-2 (Ginyu area) was drilled in an unproductive part of the reservoir; discharge from N60-KZ-2 is accompanied by a large pressure drop in the formation. It is clear from Table 4 that the "scaled maximum discharge" rate, obtained from slim hole data provides a reasonable estimate of the maximum discharge rate for large-diameter Kirishima wells with liquid feedzones. The latter result is in agreement with data from other geothermal fields discussed by Garg and Combs (1997).

Table 4. Measured and Predicted (For a 216 mm Hole) Discharge Rates For Kirishima Boreholes With Liquid Feedzones.

Borehole Name	Final Diameter (mm)	Measured Discharge (tons/hour)	Area-Scaled Discharge (tons/hour)	Scaled Maximum Discharge (tons/hour)
A. Ginyu Area — Slim Holes				
N60-KZ-2	101	6 2	28.4	43.4
KE1-3	79*	21 R	163.0	286.0
KE1-4	98	36 8	179.0	278.0
KE1-5	102	32 5	146.0	222.0
Average (N60-KZ-2 to KE1-5)			129.0	207.0
B. Ginyu Area — Intermediate Diameter				
KE1-19S	159	89.6	165.0	196.0
C. Ginyu Area — Larae Diameter				
KE1-7 (NT-C1)	216	220.0		
KE1-17 (NT-A1)	216	223.0		
KE1-22 (NT-C2)	216	233.0		
NT-A2	216	225.0		
NT-A3	216	215.0		
NT-A4	216	213.0		
NT-BI	216	231 0		
NT-B2	216	231 0		
NT-B3	216	212.0		
NT-B4	216	210 0		
Average (KE1-7 to NT-B4)		221.0		
N56-KT-8	100	42.4	198.0	304 0
KE1-11	216	313 0		

**Variable diameter hole ID is 102 mm above 900 mTVD.*

The measured maximum discharge rates for Kirishima boreholes with two-phase conditions are given in Table 5. Production from the boreholes listed in Table 5 is accompanied by a large pressure drop in the formation; this pressure drop is sufficient to cause ***in situ*** boiling. Because of ***in situ*** boiling and a large formation pressure drop, we do not expect Pritchett's scaling rule to apply to two-phase Kirishima boreholes. It is apparent from Table 5 that the "scaled maximum discharge" cannot be used to predict the discharge characteristics of large-diameter wells with two-phase feedzones based on discharge data from slim holes.

Table 5. Measured and Predicted (For a 216 mm Hole) Discharge Rates For Kirishima Boreholes With Two-Phase Feedzones.

Borehole Name	Final Diameter (mm)	Measured Discharge (tons/hour)	Area-Scaled Discharge (tons/hour)	Scaled Maximum Discharge (tons/hour)
KE1-2	75'	7 7	63 9	115 0
KE1-19	216	5 5		
KE1-21	216	17 7		
KE1-23	216	47 4		
Average (KE1-19 **to** KE1-23)		*23 5*		
C. Shiramizugoe Area — Slim Holes				
54E-OGR-1	101	4.5	20.6	31 5
N55-KT-5	101	8.0	36.6	56.0
KE1-1	78	4.9	37.6	66.5
KE1-6	98	13.5	65.6	102 0
Average (54E-OGR-1 to KE1-6)			40.1	64 0
D. Shiramizugoe Area — Large Diameter				
KE1-9	216	69.1		

**Variable diameter hole. ID is 102 mm above 802.3mTVD.*

To investigate the relationship between the discharge capacity of slim holes and large-diameter wells with two-phase feedzones, a wellbore simulator may be employed to numerically model the discharge characteristics of boreholes with different diameters. The numerical parameters derived from a fit to actual production data can then be used to investigate the effect of borehole diameter on the discharge rate. Lack of downhole pressure/temperature surveys (and hence productivity indices) for slim holes 54E-OGR-1 and N55-KT-5 and large-diameter well KE1-19 makes it impossible to perform meaningful simulations for these three boreholes. In addition, downhole pressure surveys in slim holes KE1-1 and KE1-2 were run under unsteady discharge conditions. Exclusion of the above-mentioned boreholes from the Kirishima data set leaves only one slim hole (KE1-6) and three large-diameter wells (KE1-

21, KE1-23 and KE1-9). Because of the sparseness of the Kirishima data set for boreholes with two-phase feeds, it was decided to simulate the discharge characteristics of relevant Oguni (slim hole HH-2, large-diameter well GH-15) and Sumikawa (slim hole S-2(i), and large-diameter well SA-1) boreholes as well.

MATHEMATICAL MODELING OF FLUID FLOW IN BOREHOLES WITH TWO-PHASE FEEDS

Mass and energy transport in boreholes was modeled using the wellbore computer simulation program WELBOR (Pritchett, 1985). The WELBOR code treats the steady flow of liquid water and/or steam up a borehole. The user provides parameters describing the well geometry (inside diameter and angle of deviation with respect to vertical along the hole length), a stable formation temperature distribution with depth, and an "effective thermal conductivity" (as a function of depth) representing the effect of conductive heat transfer between the fluid in the wellbore and the surrounding rock formation. Values must also be specified for the flowing feedpoint pressure (or alternately stable feedpoint pressure and productivity index) and enthalpy (or temperature for wells producing from a single phase liquid zone). For boreholes with two-phase feedzones considered here, the feedzone fluid state was prescribed by the flowing feedzone pressure and enthalpy.

In WELBOR, the frictional pressure gradient is computed using Dukler's correlation (Dukler, *et al.*, 1964) and a user prescribed roughness factor. The relative slip between the liquid and gas phases is treated using a modified version of the Hughmark liquid hold up correlation (Hughmark, 1962). The slippage rate may vary between the value given by the Hughmark correlation and no slip at all, according to the value of a user-supplied holdup parameter, η, which varies between zero (no slip) and unity (Hughmark). Numerical experimentation has shown that for a given mass flow rate the minimum pressure drop along the wellbore is obtained for an intermediate value of the holdup parameter ($0 < \eta < 1$). For most of the calculations for boreholes with two-phase feeds, it was found necessary to choose η close to its optimum value (*i.e.*, the value required to obtain the minimum pressure drop).

Most geothermal wells are completed with uncemented slotted (or perforated) liner in the open hole section of the borehole. Garg and Combs (1997) used the WELBOR code to model fluid flow in both slim holes and large-diameter wells at the Takigami Geothermal Field. All of the Takigami boreholes produce from single-phase (all liquid) feedzones. Apparently, the presence of slottedperforated liner in single-phase Takigami boreholes has little influence on fluid transport. The situation is quite different for two-phase flow. An examination of downhole pressure profiles for boreholes with two-phase feedzones shows that the pressure gradient is significantly higher in the slotted/perforated liner portion of the borehole than in the cemented and cased part of the borehole. To correctly reproduce the observed pressure gradient in the slotted/perforated liner, it was found necessary (in most cases) to assume that the inside diameter of the wellbore is equal to that of the slottedperforated liner. In addition, a non-zero pipe roughness factor for the slotted/perforated liner portion of the wellbore was used in most of the calculations presented below.

Given the downhole (usually at the uppermost feedzone) values for mass flow, pressure and enthalpy, the wellbore code can be used to compute the conditions (pressure, temperature) along the wellbore and at the wellhead (pressure, flowing enthalpy, etc.). The principal parameters that may be varied to match the measured conditions in the wellbore and at the wellhead are (1) holdup parameter η, (2) effective thermal conductivity K, and (3) interior roughness factor ε. In two-phase water/steam flow, pressure and temperature are not independent variables. For any given effective thermal conductivity K, downhole flowing enthalpy may be adjusted to yield the appropriate pressure (and hence temperature) distribution in the wellbore, and flowing wellhead enthalpy. Matching the pressure/temperature distribution in the wellbore does not constrain the flowing feedzone enthalpy and heat loss. Since the flowing feedzone enthalpy is not a measured quantity, it is difficult to determine a precise value for heat loss in the presence of two-phase flow. (The latter problem does not arise for single-phase liquid feedzones since the flowing feedzone enthalpy can be determined using the measured temperature and the steam tables.) For the above-discussed reasons, effective thermal conductivity K was eliminated as a parameter in the calculations described below, and was taken to be a constant (= 4 W/m-°C).

For both the slim holes and large-diameter wells with two-phase feedzones, WELBOR was used to match the downhole pressure/temperature profiles. The model parameters (roughness factor, holdup parameter) derived from fits to downhole data were then employed to match the results of characteristic tests by varying feedzone pressure and enthalpy. Finally the discharge characteristics of a "standard" large-diameter well were predicted using model parameters (roughness factor, holdup parameter, productivity index) for slim holes.

To illustrate the computational procedure, we consider slim hole KE1-6. The principal feedzone for Kirishima slim hole KE1-6 is located at 1235 mTVD. The stable feedzone pressure and temperature are estimated to be 73.2 bars and ~220°C, respectively. The borehole is completed with a 114 mm (103 mm ID) diameter casing cemented to a depth of 1001.2 mTVD; a 83 mm (76 mm ID) diameter uncemented liner in a 98 mm diameter hole is present from 992.3 mTVD to 1514.5

mTVD. After considerable numerical experimentation, the following well geometry was assumed for KE1-6:

Measured Depth (meters)	Vertical Depth (meters)	Angle With Vertical (degrees)	Internal Diameter (mm)
0.0 – 992.3	0.0 – 992.3	0.0	103
9923 – 1235.0	992.3 – 1235.0	0.0	76

A characteristic discharge test was performed from July 4 to July 8, 1983. The borehole discharged a mixture of water and steam with wellhead enthalpies ranging from 937 kJ/kg to 1009 kJ/kg. The measured wellhead enthalpies imply that discharge from KE1-6 was accompanied by ***in situ*** boiling. Because of the brief duration of the characteristic test, it is unlikely that stable discharge conditions were realized during the test (see below). Following the characteristic test, a downhole pressure survey was run in the discharging well on July 11, 1983. The reported discharge rate at the time of the downhole pressure surveys was considerably lower than that reported for the July 4-8, 1983 period. The measured feedzone and wellhead pressures on July 11, 1983 were 16.54 bars and 1.52 bars, respectively. Using the second order polynomial fit (see below) to the characteristic discharge data, the wellhead enthalpy corresponding to a wellhead pressure of 1.52 bars is 1009 kJ/kg.

The stable formation temperature in the vicinity of slim hole KE1-6 was specified based on measurements in the borehole. Despite considerable experimentation involving well geometry and other model parameters, it proved impossible to match the downhole pressure profile of July 11, 1983 using the reported discharge rate (10.07 tons/hour = 2.80 kg/s). Simply stated, a discharge rate of 2.80 kg/s is inconsistent with the measured pressure profile in the cased part of the borehole ***(i.e.,*** above -1000 meters). Accordingly, the discharge rate was reduced to 2.50 kg/s (*i.e.,* by about 10 percent). With a discharge rate of 2.50 kg/s, the best fit was obtained using the following model parameters:

Thermal Conductivity, K = 4 W/m°C
Holdup Parameter, η = 0.18
Roughness Factor, ε = 0 for depths <992.3 m
= 0.28 mm for depths >992.3 m
Feedzone Enthalpy, h_f = 1102kJ/kg.

The computed pressure profile, Figure 6, is in good agreement with the measurements. A discharge rate of 2.5 kg/s together with a feedzone pressure of 16.54 bars yields a productivity index of 0.044 kg/s-bar for KE1-6.

The characteristic discharge data for KE1-6 were fit using the following second order polynomials (Figure 7):

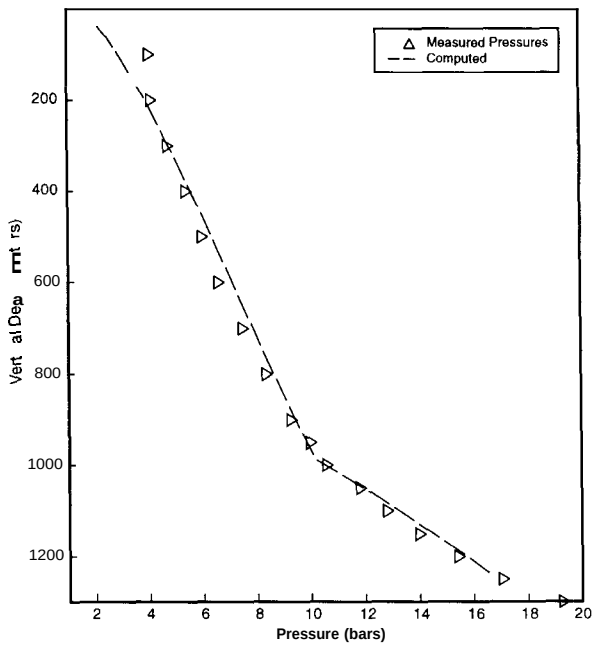

Figure 6. Pressure profile **(A)** recorded in discharging KE1-6 on July 11, 1983. The dashed line is the computed pressure profile.

$$M(\text{tons/hour}) = 17.92 - 2.928\, p_w + 0.109\, p_w^2$$
$$h_f\ (\text{kJ/kg}) = 937.4 + 85.52\, p_w - 25.38\, p_w^2$$

Model parameters (K, ε, η) obtained by fitting the downhole pressure profile were used to simulate the characteristic discharge data (indicated by a * in Figure 7). The feedzone pressure and enthalpy were varied to match the wellhead pressure and enthalpy. The results of these calculations are summarized in Table 6.

Table 6. Simulation of Characteristic Test Data for Slim Hole KE1-6.

Wellhead Pressure (bars)	Discharge Rate (kg/s)	Wellhead Enthalpy (kJ/kg)	Flowing Feedzone Pressure (bars)	Feedzone Enthalpy (kJ/kg)	Productivity Index (kg/s-bar)
1.60	3.76	1009	24.10	1112	0.0766
2.07	3.47	1007	22.54	1110	0.0685
2.39	3.20	996	20.99	1100	0.0613
2.80	2.94	978	19.59	1085	0.0548
3.20	2.69	951	18.43	1063	0.0489

The calculated results indicate that the flowing feedzone pressure increases with the discharge rate; this is contrary to general experience and implies that stable discharge conditions were not attained during the characteristic test of slim hole KE1-6.

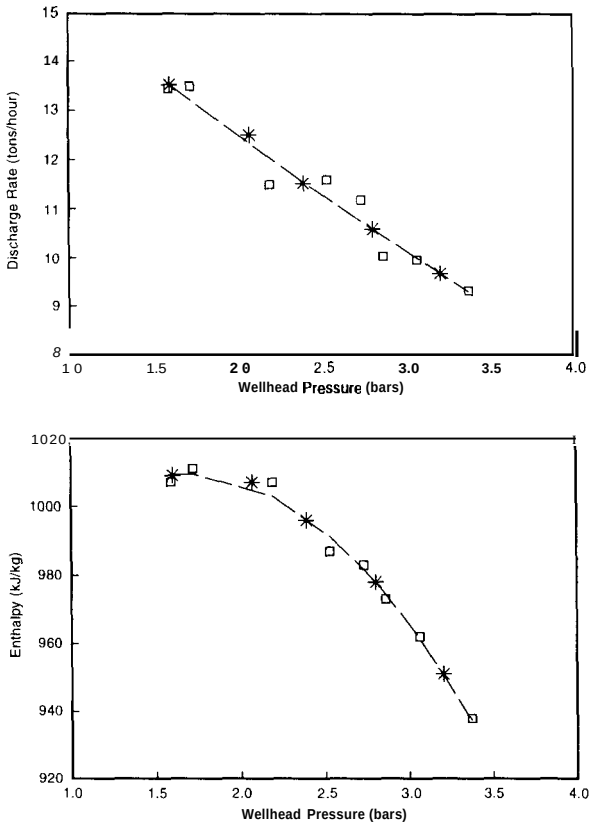

Figure 7. Discharge rate and enthalpy versus wellhead pressure for Kirishima slim hole KE1-6 (July 4-8, 1983). The dashed line indicates a second order polynomial fit to the measurements. Star (*) denotes the computed values (see text).

The model parameters (K, ε, η) for KE1-6 will next be utilized to estimate the maximum discharge rate for a typical large-diameter geothermal well (224 mm ID cased interval, 159 mm ID uncemented liner in 216 mm open hole). The following geometry is assumed for the large-diameter well:

Measured Depth (meters)	Vertical Depth (meters)	Angle With Vertical (degrees)	Internal Diameter (mm)
0–992.3	0–992.3	0.0	224
992.3 – 1235.0	992.3 – 1235.0	0.0	159

The productivity index and flowing feedzone enthalpy are taken to be 0.06 kg/s-bar and 1110 kJ/kg, respectively. Since stable discharge conditions were not obtained during the characteristic test, the productivity index for KE1-6 is poorly known; the selected value (0.06 kg/s-bar) is the median value obtained from the simulation of characteristic data (Table **6).** The choice for feedzone enthalpy (1110 kJ/kg) is about the highest value inferred from the KE1-6 discharge data. With the preceding parameter values (K, ε, η, PI, h_f) the maximum discharge rate for the large-diameter well is computed to –4.1 kg/s (*i.e.*, 14.8 tonshour).

The calculated maximum discharge rate for the large-diameter well is not much greater than that for KE1-6. Because of the very small productivity index, most of the pressure drop takes place in the formation. As far as the maximum discharge rate is concerned, the formation (and not the well diameter) is the limiting factor. Increasing the well diameter does not result in a commensurate increase in the discharge rate.

The currently available data set are not well suited for examining the effect of borehole diameter on the discharge rate. Of the five (5) large-diameter wells, four wells (KE1-9, KE1-23, GH-15 and SA-1) have productivity indices ranging from 0.2 kg/s-bar to 0.6 kg/s-bar; the maximum discharge rate for these wells varies from –36 tons/hour to –69 tons/hour. Large-diameter well KE1-21 has a productivity index of 0.06 kg/s-bar; the maximum discharge rate for this well is 17 tons/hour.

Slim hole KE1-6 has a productivity index (–0.06 kg/s-bar) similar to that for KE1-21. Using model parameters for KE1-6 the maximum discharge rate of a hypothetical large-diameter well (of a design similar to KE1-21) is predicted to be –15 tons/hour. The latter discharge rate value is in substantial agreement with the maximum discharge rate for well KE1-21. The productivity indices for the remaining two slim holes (HH-2, S-2(i)) are extremely small (–0.03 kg/s-bar). The predicted maximum discharge rates for a hypothetical large-diameter well using model parameters for HH-2 and S-2(i) are only 6 tons/hour and 5 tons/hour.

CONCLUSIONS

Production and injection test data from Kirishima boreholes with liquid feedzones support the conclusions previously derived from analyses of similar data from Oguni, Sumikawa, Takigami and Steamboat Hills Geothermal Fields (Garg and Combs, 1997). More specifically, available data from boreholes with liquid feedzones imply that (1) productivity and injectivity indices are more or less equal, and (2) discharge rate of large-diameter wells may be predicted based on test data from slim holes.

Analysis of injection and production data from boreholes with two-phase feedzones from Oguni, Sumikawa and Kirishima geothermal fields indicates that the two-phase productivity index is about an order of magnitude smaller than the injectivity index. Because of the sparseness of the data set (three slim holes and four large-diameter wells), this conclusion should be confirmed by additional data.

The detailed modeling of downhole pressure/temperature measurements and characteristic discharge data from two-phase geothermal boreholes has provided several interesting and useful insights. The pressure profile in most of the two-phase boreholes can be divided into two parts, *i.e.*, (1) cased hole, and (2) open hole or hole with a slotted liner. In most cases, the pressure gradient in the slotted liner/open hole section of the borehole is significantly greater than that in the cased part of the borehole. To model the pressure drop in the slotted liner/open hole, it is usually necessary to assume that the hole diameter is equal to the inside diameter of the liner. In addition, a non-zero roughness factor is required. Pressure data from high enthalpy wells SA-I and S-2(i) at Sumikawa suggest that the difference in gradient between the cased and open hole/slotted liner sections of the borehole declines (or even disappears) as the flow approaches single-phase steam. The latter observation is also consistent with the modeling of single-phase liquid flow in Takigami boreholes (Garg and Combs, 1997). For Takigami boreholes, the presence (or absence) of slotted liner was seen to have little influence on mass and heat transport in the wellbore.

Both the Hughmark slip correlation and the no-slip assumption give too large a pressure drop in the wellbore. Best fits to the downhole pressure/temperature data were obtained by taking a non-zero value of the holdup parameter η, *i.e.*, by taking a slip correlation in between the Hughmark and no-slip assumptions. These calculations suggest that the Hughmark correlation should be modified.

Examination of characteristic data from two boreholes at Kirishima (KE1-6, KE1-21), and one at Oguni (GH-15) indicates that it may take several days for discharge conditions to stablize in geothermal wells with two-phase feedzones. Thus, great care must be taken to obtain valid characteristic data from two-phase geothermal wells. It is simply not satisfactory to change discharge rates every few hours and expect to obtain valid characteristic data.

Simulation of characteristic data from large-diameter wells shows that both the productivity index and feedzone enthalpy undergo changes with variations in feedzone pressure and discharge rate. Lowering the feedzone pressures results in enhanced boiling and hence greater steam phase mobility. The variations in productivity index and feedzone enthalpy are, however, modest (–10 percent), and suggest that the productivity index and feedzone enthalpy corresponding to maximum discharge rate (and lowest feedzone pressure) from slim holes should be used to estimate the discharge capacity of large-diameter wells.

For boreholes with a poor productivity index, almost all of the pressure drop takes place in the formation, and increasing borehole diameter has little or no influence on the discharge capacity of the borehole. The discharge capacity for these boreholes is limited by the formation, and not by the borehole size. From the data analyzed to date, it appears that a productivity index of the order of 0.3 kg/s-bar is needed to obtain economically significant discharge rates. Data from slim hole KE1-6 and large-diameter well KE1-21 do suggest that barring variations in the productivity index with borehole diameter, it should be possible to deduce the discharge characteristics of large-diameter wells using test data from slim holes with two-phase feeds. The latter conclusion must, of course, be confirmed by data from a statistically significant number of boreholes with two-phase feedzones.

ACKNOWLEDGMENT

We express our sincere appreciation to the Nittetsu Kagoshima Geothermal Company, Ltd., Tokyo, Japan (NKGC) for their kind cooperation in making their proprietary data for the Kirishima Geothermal Field available for the present study. This work was supported by the Department of Energy Assistant Secretary for Energy Efficiency and Renewable Energy, Geothemal Program, under Contract No. AS-4910 from Sandia National Laboratories.

REFERENCES

Combs, J. and Dunn, J. C. (1992) "Geothermal Exploration and Reservoir Assessment: The Need for a U.S. Department of Energy Slim-Hole Drilling R&D Program in the 1990's" *Geothermal Resources Council Bulletin, Vol. 21, No. 10,* pp. 329-337.

Dukler, A. E., Wicks III, M. and Cleveland, R. G. (1964), "Frictional Pressure Drop in Two-Phase Flow – B. An Approach Through Similarity Analysis," *A.I.Ch.E. Journal, Vol. 10*, pp. 44-51.

Garg, **S.** K. and Combs, J. (1997), "Use of Slim Holes with Liquid Feedzones for Geothermal Reservoir Assessment," *Geothermics, Vol.* 26, pp. 153-178.

Garg, **S.** K., Combs, J. and Abe, M. (1995), **"A** Study of Production/Injection Data From Slim Holes and Large-Diameter Production Wells at the Oguni Geothermal Field, Japan," *Proceedings World Geothermal Congress,* Florence, Italy, May 18-31, pp. 1861-1868.

Gokou, K., Miyashita, A. and Abe, I. (1988), "Geologic Model of the Ginyu Reservoir in the Kirishima Geothermal Field, Southern Kyushu, Japan," *Proceed-*

ings International Symposium on Geothermal Energy, Exploration and Development of Geothermal Resources, Kumamoto and Beppu, Japan, Nov. 10-14, pp. 132-135.

Hadgu, T., Zimmermann, R. W. and Bodvarsson, G. S. (1994), "Theoretical Studies of Flowrates from Slim Holes and Production-Size Geothermal Wells,'' *Proceedings Nineteenth Workshop on Geothermal Reservoir Engineering,* Stanford Univeristy, Stanford, California, January 18-20, pp. 253-260.

Hughmark, G. A. (1962), "Holdup in Gas-Liquid Flow," *Chemical Engineering Progress,* Vol. 53, pp. 62-65.

Kitamura, H., Ishido, T., Miyazaki, S., Abe, I., and Nobumoto, R. (1988), "NEDO's Project on Geothermal Reservoir Engineering – A Reservoir Engineering Study of the Kirishima Field, Japan," *Proceedings Thirteenth Workshop on Geothermal Reservoir Engineering,* Stanford University, Stanford, CA, January 19-21, pp. 47-51.

Kodama, M., and Gokou, K. (1995), "Achievement Ratio of Drilling Wells in the Kirishima Geothermal Field, Japan," *Proceedings World Geothermal Congress,* Florence, Italy, May 18-31, pp. 1479-1484.

Kodama, M., and Nakajima, T. (1988), "Exploration and Exploitation of the Kirishima Geothermal Field," *Chinetsu,* Vol. 25, pp. 1-30 (in Japanese).

Pritchett, J. W. (1985), "WELBOR: **A** Computer Program for Calculating Flow in a Producing Geothermal Well," Report No. SSS-R-85-7283, S-Cubed, La Jolla, California.

Pritchett, J. W. (1993), "Preliminary Study of Discharge Characteristics of Slim Holes Compared to Production Wells in Liquid-Dominated Geothermal Reservoirs," *Proceedings Eighteenth Workshop on Geothermal Reservoir Engineering,* Stanford University, Stanford, California, January 26-28, pp. 181-187.

Saga, **Y.** and Nobumoto, R. (1988), "Kirishima Geothermal Area," *Geothermal Fields and Geothermal Power Plants in Japan, International Symposium on Geothermal Energy, Exploration and Development of Geothermal Resources,* Kumamoto and Beppu, Japan, Nov. 10-14, pp. 125-132.

Shimizu, A., Misu, S., and Gokou, K. (1988), "Geochemical Studies of the Ginyu Reservoir in the Kirishima Geothermal Field," *Proceedings International Symposium on Geothermal Energy, Exploration and Development of Geothermal Resources,* Kumamoto and Beppu, Japan, Nov. 10-14, pp. 136-139.